Invited Article: Visualisation of extreme value events in optical communications

Stanislav Derevyanko, Alexey Redyuk, Sergey Vergeles, and Sergei Turitsyn

Citation: APL Photonics **3**, 060801 (2018); doi: 10.1063/1.5026986
View online: https://doi.org/10.1063/1.5026986
View Table of Contents: http://aip.scitation.org/toc/app/3/6
Published by the American Institute of Physics

Invited Article: Visualisation of extreme value events in optical communications

Stanislav Derevyanko,[1,a] Alexey Redyuk,[2,3,b] Sergey Vergeles,[4,5] and Sergei Turitsyn[2,6,c]
[1]*Department of Electrical and Computer Engineering, Ben Gurion University of the Negev, Beer Sheva 84105, Israel*
[2]*Novosibirsk State University, Novosibirsk 630090, Russia*
[3]*Institute of Computational Technologies SB RAS, Novosibirsk 630090, Russia*
[4]*Landau Institute for Theoretical Physics RAS, Moscow 119334, Russia*
[5]*Moscow Institute of Physics and Technology, Dolgoprudnyj 141700, Russia*
[6]*Aston Institute of Photonic Technologies, Aston University, B4 7ET Birmingham, United Kingdom*

(Received 26 February 2018; accepted 2 May 2018; published online 22 May 2018)

Fluctuations of a temporal signal propagating along long-haul transoceanic scale fiber links can be visualised in the spatio-temporal domain drawing visual analogy with ocean waves. Substantial overlapping of information symbols or use of multi-frequency signals leads to strong statistical deviations of local peak power from an average signal power level. We consider long-haul optical communication systems from this unusual angle, treating them as physical systems with a huge number of random statistical events, including extreme value fluctuations that potentially might affect the quality of data transmission. We apply the well-established concepts of adaptive wavefront shaping used in imaging through turbid medium to detect the detrimental phase modulated sequences in optical communications that can cause extreme power outages (rare optical waves of ultra-high amplitude) during propagation down the ultra-long fiber line. We illustrate the concept by a theoretical analysis of rare events of high-intensity fluctuations—optical freak waves, taking as an example an increasingly popular optical frequency division multiplexing data format where the problem of high peak to average power ratio is the most acute. We also show how such short living extreme value spikes in the optical data streams are affected by nonlinearity and demonstrate the negative impact of such events on the system performance. https://doi.org/10.1063/1.5026986

INTRODUCTION

The idea that an information-bearing signal can be treated as a random process was pioneered and promulgated by Wiener and Shannon back in the 1940s of the previous century. Each information-carrying optical signal features statistical distributions of the power (intensity) and phase, varying with modulation formats and coding.[1] The statistical properties of the data-generated random process have a direct impact on transmission of information. When the distribution of power is characterised by high frequency of occurrence of large (compared to the average power level) fluctuations,[2] signal transmission becomes sensitive to the nonlinear properties of channel and/or nonlinear devices used in signal processing. Fast speed of optical processing and the corresponding possibility of observation

[a]E-mail: stasd@bgu.ac.il
[b]E-mail: alexey.redyuk@gmail.com
[c]E-mail: s.k.turitsyn@aston.ac.uk

of a large amount of realisations make statistical properties important in various practical applications such as, e.g., optical communications and lasers.

On a separate front, recently, there has been a surge of papers and monographs studying analogies between waves in hydrodynamics and optics, with a special focus on optical rogue waves (see, e.g., Refs. 3–10 and numerous references therein). Mathematical models describing irregular, random dynamics of a multitude of spectral modes are similar for certain classes of hydrodynamic turbulence and optical wave turbulence (see, e.g., Refs. 11–15 and references therein). In many practically important problems in the area of photonics, nonlinearity plays a key role in the formation of statistically rare waves of high amplitude. This is reflected in a number of publications on nonlinear optical rogue waves in various physical systems. There are, however, other possibilities for the formation of ultra-high amplitude waves that should not be overlooked. In particular, similar to the ocean science,[3,4] there exist *completely linear mechanisms* of occurrence of such freak optical waves.[16] Such mechanisms are based on dispersive wave dynamics and statistically rare co-phasing leading to appearance of huge amplitude linear wave packet. This situation is especially relevant in modern coherent optical communication systems using phase for information coding.

Optical signal $E_0(t) = E(t, z = 0)$ carrying information is characterised by statistical distributions that change with distance, as the signal propagates along the optical fiber. Signal properties are affected by fiber communication channel loss/gain, dispersion and nonlinear effects. Statistical fluctuations in telecommunication data streams occur both due to the information content of the optical signal and overlapping of many symbols. Exploitation of optical phase and multi-level data coding in coherent communication systems leads to very irregular waveforms with substantial statistical variance of power (high peak-to-average-power ratio).[2] Therefore, transmission of information in modern fiber-optic links is strongly dependent on statistical characteristics of the propagating signal. The propagation of the random function corresponding to the initial signal along the fiber (along spatial coordinate z) creates a random process in the (z, t) plane. Visually, the intensity of such an information signal $I(z, t) = |E(z, t)|^2$ presents random dynamics of two-dimensional waves, and as such, has a certain degree of similarities with ocean waves. The analogy between waves in optical fiber and in the ocean has been discussed already and many remarkable similarities have been reported.[5,13,17,18] One of the important features of the ocean waves is a huge scale of a physical system where waves appear. In terms of statistics, this may be considered as an extremely large number of realisations that make potentially observable even rare events. Modeling of ocean waves or their optical analogies in laboratory experiments lacks this statistical aspect that may be compensated by bias toward specific regimes and increased probabilities of certain fluctuations and nonlinear effects. Here we would like to point out that there are optical systems with scales comparable with the ocean both in terms of physical size and statistical properties. Indeed, transoceanic optical fiber links have a spatial scale of the ocean, and the temporal domain variations might produce an ultra-large number of statistical events due to the ultra-fast properties of photonics. In this sense, a two-dimensional information signal $I(z, t) = |E(z, t)|^2$ propagating through transoceanic optical links offers statistical realisations well beyond what can be observed in the laboratory and comparable in some ways in numbers with the huge statistics of ocean waves. In optical transmission, similar to ocean, waves are not pre-designed intentionally, but occur due to natural course. This, of course, does not exclude a possibility to create some special statistically rare events in fiber-optic light propagation on purpose. Here we present results of numerical modeling supporting this analogy and exact analytical results concerning rare statistical spatio-temporal fluctuations of intensity.

We will focus in this work on identifying dangerous phase-coded sequences that lead to those rare events. Rather than dealing with the probabilistic approach of tracking each and every wave in the "photonic ocean" (which may take a lot of realizations), we are effectively "seeding the storm," i.e., calculating analytically the initial phase patterns that generate the freak wave at a given point of the fiber. To achieve that goal we have transferred here some well-known methods of diffraction optics to the field of optical communications presenting a concept of "engineered" digital freak waves. Knowledge of such patterns leading to large amplitude fluctuations at the non-desirable points (nonlinear elements, amplifiers, and so on) can be used in signal coding,[19] effectively removing the most dangerous combinations.

In this paper, we have concentrated on linear systems with uncompensated chromatic dispersion; such systems are becoming increasingly popular because of the advent of electronic dispersion compensation.[20] Their advantage is the suppression of cross-phase modulation, due to the large walk-off between wavelength channels, but they could suffer from high peaks in power. It is exactly these effects that we are trying to describe here. At the end of the section titled "Results and Discussion," we also study the impact of fiber nonlinearity and noise on the properties of such telecom freak waves as well as the impact of the latter on system's performance.

MATERIALS AND METHODS

Wavefront shaping methods in the imaging through turbid media

Since we will use a mathematical approach from the diffraction optics, in this section, we give a brief self-contained overview of the recent developments in this field. Recent years have seen a breakthrough in the area of optical imaging in disordered media via the so-called "adaptive wavefront shaping"—see Refs. 21–24 and the recent review.[25] The original idea of the method is due to the work of Vellekoop and Mosk[21] who used the spatial light modulator (SLM) to control the phases of different areas of the impinging optical beam in such a way as to achieve maximum constructive interference of different optical paths at a given observation point. Using the phases of a (large) number of SLM pixels as effective controllable degrees of freedom, they were able to focus light even in the case when the beam passes through a disordered medium (a diffuser) and when the non-optimized wavefront produces just a random speckle pattern with a uniform average intensity profile.[26]

Mathematically the optical field at the point of interest in the observation plane can be presented as a linear superposition of the fields from each individual pixel,

$$E = \sum_{n=1}^{N} \tilde{t}_n r_n e^{i\phi_n}, \tag{1}$$

where r_n and ϕ_n are the amplitude and phase of light reflected from the nth SLM pixel and N is the total number of pixels. In most application, a phase-only SLM matrix is used meaning that one has full control over the phases ϕ_n only while the amplitudes r_n are just the amplitudes of the initial beam averaged over the nth SLM pixel. As the input beam is usually very broad (much larger than the size of the SLM matrix), one can assume that the intensity front at the SLM is uniform, i.e., $r_n = r_0$, where the constant r_0 is related to the total power of the incident wave.

The set of *transmission coefficients* $\{\tilde{t}_n\}_{n=1}^{N}$ contains all the information about the linear propagation of the signal from a given SLM pixel to the destination. Generally these coefficients are a set of random uncorrelated complex Gaussian variates and one can borrow from the well-established machinery of the random matrix theory to describe their statistical properties. As was realized by Vellekoop and Mosk the intensity corresponding to the field (1), $I = |E|^2$ reaches its maximum when the SLM phases are conjugated with respect to the phases of the corresponding transmission coefficients:

$$\phi_n = -\mathrm{Arg}[\tilde{t}_n]. \tag{2}$$

Indeed in this case all the terms in the sum (1) are *in phase* and the magnitude of the resulting complex vector is maximal. It is easy to show that in the case of the disordered uncorrelated paths the average enhancement over the non-optimized background (i.e., the average speckle field) scales as the number of pixels, N.[21,22] In the deterministic case, the set of the transmission coefficients can in principle be obtained analytically if the Green function is known. In the optical imaging applications, this is rarely the case, especially when considering the imaging through disordered medium as multiple photon scattering makes any deterministic description impossible. In this case, one has to resort to real-time optimization of the phase mask $\{\phi_n\}_{n=1}^{N}$ using the current value of the intensity I at the target plane as a feedback for the optimization algorithm (see Refs. 21, 22, and 25 for details), and both spatial and temporal focusing can be achieved.[24] The usual method of choice for the wavefront shaping imaging is the so-called genetic algorithm (see, e.g., Ref. 27) but of course one can use other continuous optimization methods as well.

Data streams in optical telecommunications

Let us now outline the main mathematical model we will be using in the subsequent analysis of optical communication data streams and its connection to the imaging problem from the section titled "Wavefront shaping methods in the imaging through turbid media". We will focus without loss of generality on the well-known and practically important example—orthogonal-frequency-division-multiplexing (OFDM) that is the modulation technique of choice in a number of communication applications.[2] Although OFDM is widely known and used in wireless communication systems, in the last decade we observe an explosive growth of research related to OFDM in optical communications. The major advantages of OFDM are elimination of intersymbol interference caused by a dispersive channel and moving the complexity of transponders from the analog to the digital domain. This becomes increasingly important for long-haul fiber systems as data rates continue to grow. For illustrative purposes, we shall also provide results for single carrier Gaussian-shaped pulse return-to-zero format which, although less relevant to modern day optical communication systems, admits full analytical treatment. The communication signal is built as an overlap of a large number of statistically independent information subcarriers. By design, the OFDM signal is prone to statistical fluctuations of power that are characterised by engineers in terms of the so-called peak-to-average power ratio (PAPR). We would like to refer to a comprehensive and excellent review[28] for the general introduction to the problem of PAPR and its reduction in wireless communications. The distribution of PAPR bears the imprint of the stochastic characteristics in OFDM systems.[29,30] High amplitude fluctuations make OFDM transmission sensitive to any nonlinear effects that occur in the channel or in the nonlinear devices used in its signal processing loop. For instance, if a high amplitude fluctuation occurs before or at a high power amplifier this severely impairs system performance. The signal launched into fiber links can be presented as

$$E(z=0,t)=\sum_{\alpha=1}^{N_{sc}}\sum_{n=1}^{N} c_{n\alpha}s(t-nT_s)e^{2\pi i f_\alpha t}, \tag{3}$$

where N is the total number of symbols, $c_{n\alpha}$ are the set of the modulation symbols, $1/T_s$ is a given symbol rate, $s(t)$ is the shape of the envelope carrier (assumed here the same for each symbol for simplicity) and additionally to include the popular orthogonal multicarrier formats (OFDM or Nyquist) we have also introduced the sum over a finite set of N_{sc} equispaced subcarriers $f_{\alpha+1}-f_\alpha = 1/T_s$ (see, e.g., Refs. 2 and 31).

In what follows, we shall assume phase only modulation schemes in which the $c_{n\alpha}$ are drawn from a series of given circles of fixed radii $|c_{n\alpha}| \in \{r^{(1)}, r^{(2)}, \ldots, r^{(M)}\}$. This corresponds to a popular *ring constellation* format[32] for the continuous case or M-PSK phase-shift key modulation in the discrete case.[1] In what follows, we will assume that the radius $|c_{n\alpha}| = \sqrt{S}$ is given and concentrate on the phases $\phi_{n\alpha} = \mathrm{Arg}[c_{n\alpha}]$ of each symbol. Traditionally in the phase-shift keying (PSK) format, these phases form equidistant vertices of a certain polygon on each ring but we will assume for now that they can take arbitrary values for each symbol in the interval $[0, 2\pi]$.

After the propagation in the long span of optical fiber, the pulses experience strong overlap as well as dispersion-induced shift specific for any multicarrier format.[2] This temporal shift, $t_d(\alpha)$, is usually compensated via the cyclic prefix method, where a guard band of length $\Delta_G > \max_\alpha[t_d(\alpha)]$ is inserted inside each slot and the leading part of the carrier is copied into this band before transmission.

Mathematically the output field can be presented as

$$\begin{aligned} E(z=L,t) &= \sum_{\alpha=1}^{N_{sc}}\sum_{n=1}^{N} \tilde{t}_{n\alpha}(L,t) r_{n\alpha} e^{i\phi_{n\alpha}}, \\ \tilde{t}_{n\alpha}(L,t) &\equiv \int dt' G(L, t-nT_s-t') s(t') e^{2\pi i f_\alpha t'}, \end{aligned} \tag{4}$$

where G is a well-known Green function of the dispersive propagation (see the supplementary material for details).

One can see now the full equivalence of the imaging problem of diffraction optics [Eq. (1)] and the propagation of the phase modulated sequence of multi-carrier pulses. Schematically, we can

reflect this correspondence as "pixels" ⇔ "symbols," "phase mask" ⇔ "phase-encoded message." Using phase conjugation recipe given by Eq. (2) with the "transmission coefficients" given by Eq. (4), one can identify the most dangerous phase combination leading to a coherent enhancement of a field at a given time mark and a given point in a fiber forming a *linear rogue wave* (RW) (compared to ocean waves[3]) in the optical data stream.

In this paper, we concentrate on the two most basic effects of fiber propagation: second order dispersion and loss. One could in principle include other linear effects such as higher order dispersion, polarization mode dispersion, etc. While this is an important task for the future study, we note here that this would only affect the analytical form of the Green function G in Eq. (4). While this will certainly have an impact on the shape of the resulting rogue wave, it will not change the *main mechanism* of their formation as discussed above: namely, coherent superposition of multiple symbols when the initial phases meet the resonance condition (2).

RESULTS AND DISCUSSION

The power enhancement and the shape of a linear digital freak wave. Theory

In the field of imaging through turbid media, the main figure of merit for each given method is the so-called enhancement: namely, the ratio of the maximum intensity achieved at the desired focus point to the average background formed by a nonoptimized, incoherent contribution of different sources.[21,22] In the optical telecommunication applications, this enhancement can readily be recognised as the PAPR discussed in the section titled "Materials and methods". In order to emphasize the connection between these two seemingly different areas of optics, we shall use these terms interchangeably. In what follows, we shall assume that the total accumulated dispersion in the fiber $B(L) = \int_0^L \beta_2(z)dz$ is large (see the supplementary material). Here $\beta_2(z)$ is the second order dispersion coefficient. We are assuming here the case of the uncompensated communication links with no pre-chirping as these schemes are becoming increasingly popular in modern day optical communications due to the advent of the coherent detection with digital signal-processing (DSP).[20] To gauge the strength of the dispersion-induced overlap, we introduce the large parameter $\varphi = |B(L)|/T_s^2 \gg 1$. Then not only the different subcarriers in the same slot can interfere constructively (as is usually assumed in the classic OFDM problems[2]), but also pulses from different slots can overlap providing additional degrees of freedom for enhancement. From the expressions (1) [or rather its telecom equivalent (4)] and (2), we arrive at the following result for the power enhancement, i.e., PAPR, η:

$$\eta = \frac{\left(\sum_{\alpha=1}^{N_{sc}} \sum_{n=1}^{N} |\tilde{t}_{n\alpha}|\right)^2}{\sum_{\alpha=1}^{N_{sc}} \sum_{n=1}^{N} |\tilde{t}_{n\alpha}|^2} \equiv \varphi \Omega[N_{sc}, N/\varphi], \quad \varphi \gg 1. \tag{5}$$

Simply put the above result says that the enhancement is proportional to the total amount of phase degrees of freedom that can effectively contribute to the phasor sum (4). This number of degrees of freedom is proportional to overlap parameter φ but also contains an additional form-factor Ω which takes into account the finite number of pulses and subcarriers. When the number of subcarriers is not too large (precise condition will be given below) or if one uses cyclic prefix to prevent the dispersion-induced walk-off, the sums over subcarriers in (5) scale linearly with N_{sc} and one can write $\Omega[N_{sc}, N/\varphi] \approx N_{sc}\Omega_0[N/\varphi]$. The new form factor Ω_0 has a sharp cutoff when the argument becomes less than unity (so that the number of contributing degrees of freedom for each subcarrier is bound from above by the total number of pulses) while its behavior in the practically relevant cases of large sequences $N \gg \varphi$ must be determined for each particular modulation format and the carrier shape. The problem has been previously studied in Ref. 16 in a special case of a large number of single carrier Gaussian pulses (see also the supplementary material). There it was obtained that $\Omega_0[N/\varphi] \sim 1$ when $N \gg \varphi$. However the dispersive propagation of Gaussian pulses has one particular property that the pulses keep their shape, i.e., remain well localized. As we shall see below the rectangular shape of the OFDM, carrier changes this simple result. We show, in particular, that the problem is equivalent to 1D

lens imaging of the square aperture which has a well-known oscillating Fresnel solutions with slow decay. Because of that the effective overlap between the dispersing pulses becomes even stronger which makes PAPR significantly higher. In this section, our goal will be to calculate theoretically the resulting PAPR as well as obtain the shape of the telecom freak wave.

To get some analytical results, we use simplified expressions for the transmission coefficients in Eq. (4) derived in the supplementary material in the limit $\varphi \gg 1$ and neglecting the cyclic prefix. Using the already mentioned analogy with the diffraction optics, the approximation made is exactly equivalent to that in the Fraunhofer diffraction limit which is the basis of the so-called Fourier optics.[33] We note of course that the formal analogy between paraxial diffraction and space and dispersion in time is well known giving rise to the concept of "time lens."[34,35] Here we are simply using this analogy to extract the phases of the encoded symbols. Omitting the details of the calculation (see the supplementary material), one gets the following expressions for the optimal phases of each symbol and the temporal shape near the focus $t = t_*$:

$$\begin{aligned}
\phi_{n\alpha} &\approx -\mathrm{Arg}[\tilde{s}_{n\alpha}(t_*)] + \frac{nT_s(nT_s - 2t_*)}{2B(L)},\\
P_{opt}(t) &\approx \frac{2S\varphi}{\pi}|g_0(t-t_*)|^2 \frac{\sin^2\left[\dfrac{\pi N_{sc}(t-t_*)}{T_s}\right]}{\sin^2\left[\dfrac{\pi(t-t_*)}{T_s}\right]},\\
g_0(\Delta t) &\equiv \int\limits_{t_*T_s/(2B(L))}^{(t_*-NT_s)T_s/(2B(L))} dy e^{-2iy\Delta t/T_s}\left|\frac{\sin y}{y}\right|,
\end{aligned} \tag{6}$$

where $\tilde{s}_{n\alpha}$ is the Fourier transform of the carrier shape evaluated at the argument $f_\alpha + (t - nTs)/(2\pi B(L))$ and in the second line, we have additionally assumed that $\varphi \ll N/N_{sc}$. The width of the temporal focus at $z = L$ appears to be $\Delta t \sim T_s/N_{sc}$ in this regime. The full spatio-temporal shape of the emerging RW can also be obtained analytically (see the supplementary material). In particular at the point $t = t_*$ and when $N_{sc}^2|B(z) - B(L)| \ll T_s^2$, the spatial shape of the RW is again given by the second line in Eq. (6), where one must substitute $t_*(B(z) - B(L))/B(L)$ for $t - t_*$. For the case of constant second order dispersion β_2 assuming that the sampling is made in the middle of the original sequence, $t_* = (N/2)T_s$, the width of the spatial focus is given by $\Delta z = \min[L_D, 4L/(NN_{sc})]$, where $L_D = T_s^2/|\beta_2|$ is the dispersion length.

From (6) assuming $t_* = (N/2)T_s$, the PAPR of Eq. (5) is expressed as

$$\eta = \varphi\Omega[N_{sc}, N/\varphi] = N_{sc}\varphi \frac{2\left(\displaystyle\int\limits_{-N/4\varphi}^{N/4\varphi}\left|\frac{\sin y}{y}\right|dy\right)^2}{\displaystyle\int\limits_{-N/4\varphi}^{N/4\varphi}\frac{\sin^2 y}{y^2}dy}, N \gg N_{sc}\varphi \tag{7}$$

(see the supplementary material for details). Let us estimate the lower and upper bounds for the obtained PAPR. To get the lower bound, one replaces $|\sin y/y|$ with $\sin y/y$, and in the considered limit, $N \gg \varphi$ also replaces the integration boundaries with the infinite ones. The resulting lower bound is $\eta_< = 2N_{sc}\varphi$. The upper bound is obtained immediately by virtue of the Cauchy-Schwarz inequality which yields $\eta_> = NN_{sc}$. In reality, the relative enhancement η grows very slowly (logarithmically) with N/φ due to large dispersive overlap of the carrier shapes.

The numerical results and visualisation of spatio-temporal dynamics of telecommunication data streams

Note that the theoretical results from the section titled "The power enhancement and the shape of a linear digital freak wave. Theory," concern continuous phase distribution of the input symbols, i.e., ring constellations.[32] In digital communications, of course, one uses the discrete phase shifted

(M-PSK) constellation scheme, where the phases $\phi_{n\alpha}$ are not arbitrary, but sampled from a discrete set of M values. In this case, the optimal phases prescribed by Eq. (2) may not actually be close to the allowed constellation points. As mentioned in Sec. II in the imaging through disordered media, the precise values of the transmission coefficients are unknown and one resorts to the full optimization of the optimal phase mask. In principle, one must do the same in the telecom problem, namely, run a discrete optimization algorithm in the discrete space of $M^{N\times N_{sc}}$ allowable phase permutations. Here we demonstrate that such drastic measures are not necessary and one can successfully use the optimal continuous phases as given by theory (2) and (4) and then find the closest constellation point.

In this section, we compare the results of the developed theory with full numerical simulations of the signal propagation. We use the standard split-step Fourier propagation scheme[36] although strictly speaking it is only fully used in section titled "The effect of nonlinearity on linear freak waves" dedicated to the nonlinear effects. In the rest of the simulation, the propagation was modelled by a single step in the Fourier domain.

Single carrier RZ Gaussian pulses

To illustrate the basic concept of the "photonic ocean," we first provide the numerical results for the single carrier Gaussian-shaped pulse stream. Figure 1 visualizes a typical spatio-temporal dynamics (evolution with distance of the temporal power distribution) of the binary phase-shift keying (BPSK) signal $[A(t, z=0) = \sum_k c_k f(t - kT_s)$ with $\mathrm{Arg}[c_k]$ selected from two possible values $\{0, \pi\}$; here $f(t) = \exp\left(-t^2/2\tau^2\right)$ is Gaussian pulse in the figure below] in standard single-mode optical fiber based coherent transmission links. The initial optical signal represents a sequence of single carrier Gaussian pulses with fixed input pulse profile $f(t)$, $\tau = 2$ ps, fixed input power $S = |c_k|^2 = 1$ mW,

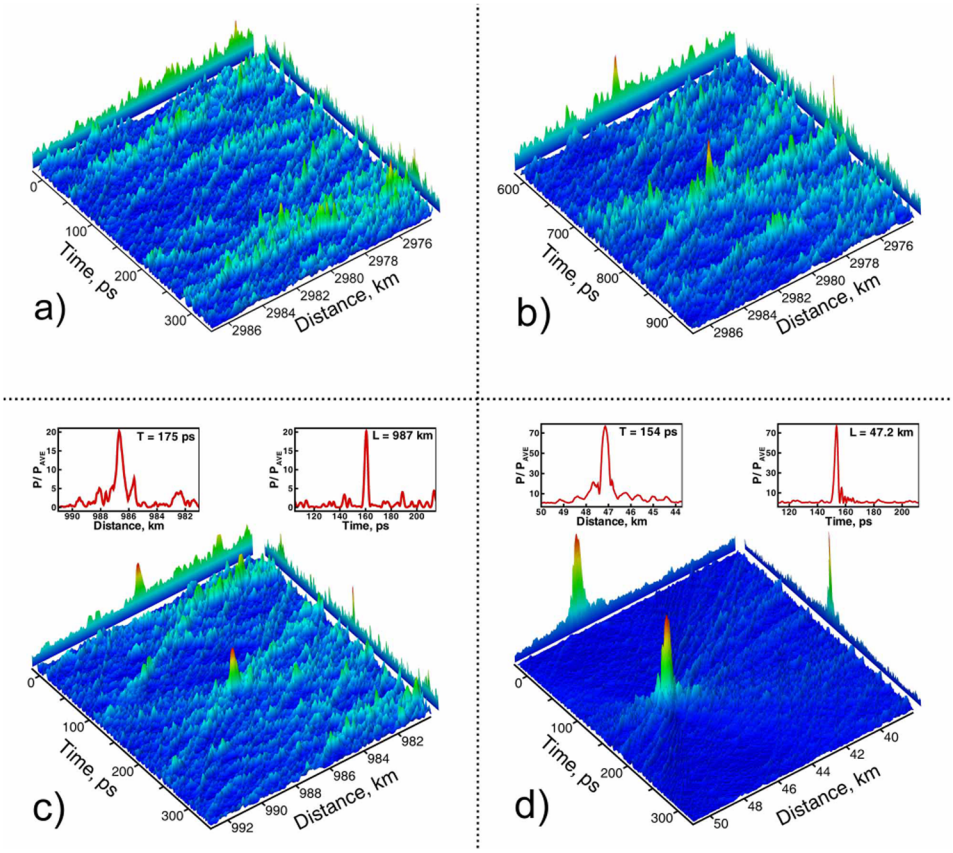

FIG. 1. Two-dimensional visualisation (spatio-temporal dynamics) of the waves in the data streams transmitted in the fiber-optic links: (a) low amplitude waves, (b) "windy" wave regime, (c) "storming" wave regime, and (d) appearance of "digital freak wave." The insets show the spatial and temporal cross-sections of the intensity peak.

and repetition rate 100 GHz (T_s = 10 ps). The periodic section of transmission links consists of 100-km span of the standard single-mode fiber ($\beta_2 = -20.4$ ps^2/km and $\alpha = 0.2$ dB/km) followed by the amplifier. The simulation of signal propagation along the fiber was performed using the linear Schrödinger model (see the supplementary material).

There are various characteristic regimes that demonstrate similarity with wave behavior in the ocean. Figure 1(a) illustrates the dominant regime of low amplitude waves, when a large number of pulses from different slots, phase modulated by random binary sequence, broaden and overlap forming spatio-temporal dynamics with moderate amplitude fluctuations. Figures 1(b) and 1(c) show examples of the "windy" and "storming" wave regime, respectively, which occur more rarely than low amplitude waves because of decreased probabilities of certain fluctuations. Figures 1(a)–1(c) represent particular realizations of the field propagation corresponding to different pseudo-randomly generated input phase sequences. By contrast, Fig. 1(d) demonstrates the appearance of linear optical freak wave as a result of an overlap of a number of pulses, obtained by the pre-engineered input phase sequence given by Eq. (2) and rounded to the nearest phase level. Although the latter detrimental phase modulated sequence was obtained analytically, it is still random in sense of information content and can freely occur in a transmitted data stream.

The OFDM simulations

Finally, we present here the results of the rogue wave generation from OFDM signals. First, we verify the theoretical predictions of the structure of such fluctuations by numerical calculations assuming quasi-linear dynamics to make the nature of the effect clear (impact of nonlinearity is considered separately in the section titled "The effect of nonlinearity on linear freak waves") and set the parameters as follows: the average signal power of each subcarrier $S = |c_k|^2 = 1$ mW, $T_s = 25$ ps, $\beta_2 = -20.4$ ps^2/km, and $L = 4000$ km. As a result, we held φ fixed and varied number of symbols, N, and subcarriers, N_{sc}. Without loss of generality, we will assume that transmission link is quasi-lossless, when gain exactly compensates for the fiber losses. This corresponds to either path-average model or by a special distributed Raman amplification scheme. The simplified propagation model in this section is obtained by taking the more general equation (8) below and setting the Kerr coefficient to zero (which is justified when dispersion length is much smaller than nonlinearity length, both defined in the following).

As follows from Eq. (6) for a single subcarrier, the temporal shape of the RW is determined by the temporal shape of g_0 which has the typical focus width $\Delta t \sim T_s$ for large enough values of N/φ. Full temporal shape of the RW, obtained analytically by Eq. (6) and through numerical simulation for different values of the parameter N/φ for the fully symmetric location $t_* = (N/2)T_s$, is shown in Fig. 2. It can be seen that there is a close agreement between the theory and the numerics. It should

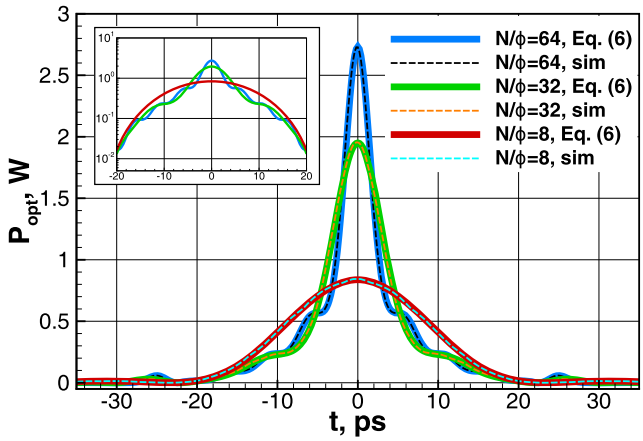

FIG. 2. Comparison of analytic expression given by Eq. (6) (solid lines) and numerical simulation (dashed lines) of temporal shape near the focus for different values of the parameter N/φ for the fully symmetric location $t_* = (N/2)T_s$. Inset: temporal shape in the log scale.

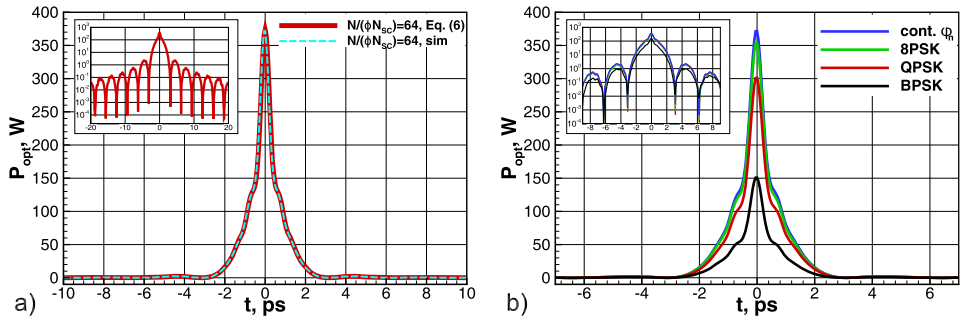

FIG. 3. The shape of multi-carrier focus obtained by analytic expression given by Eq. (6) (solid lines) and numerical simulation (dashed lines) for $N_{sc} = 8$ (a). The shape of multi-carrier focus for continuous and discrete M-PSK ($M = 2$, 4 and 8) phase distribution of the input symbols (b). Insets: temporal shapes are on a log scale.

also be noted that even in the case of single subcarrier we observed some dramatic values of PAPR of the order of 2700 (when $N/\varphi \approx 64$).

For multiple subcarriers, there is an additional oscillating prefactor, producing tail oscillations, as shown in the inset of Fig. 3(a) for $N_{sc} = 8$. In this case, the width of the temporal focus at $z = L$ is given by $\Delta t \sim T_s/N_{sc}$ in regime $N \gg N_{sc}\varphi$. As follows from Eq. (6), peak power of the RW scales as N_{sc}^2 that is confirmed by our simulations. Considering that average power is linearly proportional to the number of subcarriers, we immediately obtain linear dependence of PAPR on N_{sc}. Again there is a close agreement between theory and simulation as in the single-carrier case. Figure 3(b) demonstrates temporal shape of RW for continuous and discrete phase distributions of the input symbols. Discrete phase distributions were obtained using the optimal continuous phases by finding the closest constellation point from a discrete set of M values, where $M = 2$, 4 and 8. As is seen, this method not only works for the dense format ($M = 8$) but also for the relatively sparse one like BPSK ($M = 2$) and QPSK (i.e., M-PSK with $M = 4$). Of course strictly speaking, the RW generated for the latter two formats is suboptimal due to large truncation error; however Fig. 3 clearly demonstrates that such "suboptimal" sequences can lead to significant PAPR.

Finally, Fig. 4 shows full spatio-temporal dynamics of the rogue waves risen in the transmitted BPSK modulated sequence of pulses for parameters listed above.

Apart from the well pronounced temporal tail oscillations due to multiple subcarriers, the shape of the focus appears to be rotated in the (t, z) plane—an apparent consequence of the neglected phase prefix and dispersion walk-off for each subcarrier.

The effect of nonlinearity on linear freak waves

An important issue from both fundamental and practical point of view is the impact of nonlinear effects on the generation of linear freak waves because channel nonlinearity is not negligible in long-haul fiber systems. To investigate the contribution of nonlinearity to a completely linear mechanism of occurrence of such waves, we consider the nonlinear Schrödinger equation as a master model,[36]

$$\frac{\partial E}{\partial z} + i\frac{\beta_2}{2}\frac{\partial^2 E}{\partial t^2} - i\gamma|E|^2 E = 0, \tag{8}$$

where β_2 is the dispersive term and γ is the nonlinear term. We consider here without loss of generality and similar to[32] a lossless model that corresponds to either path-average description or a quasi-lossless second-order distributed Raman amplification scheme.[37] We solve Eq. (8) numerically by using the well-known split-step Fourier method. The value of channel parameters was chosen as $\beta_2 = -20.4$ ps^2/km, and $\gamma = 1.3$ (W km)$^{-1}$, corresponding to the standard communication fiber. Symbol period T_S is 25 ps and the distance of freak wave appearance L is 2000 km.

To change signal propagation mode from linear to nonlinear, we vary input average signal power P_0. The nonlinearity is customary gauged not by the power level alone but by the so-called nonlinear length $L_{NL} = (\gamma P_0)^{-1}$ and its relation to the dispersion length L_D.[36] To begin with, we suppose that the phase of each symbol is continuous as given by (2) and (4). Figure 5 shows spatio-temporal

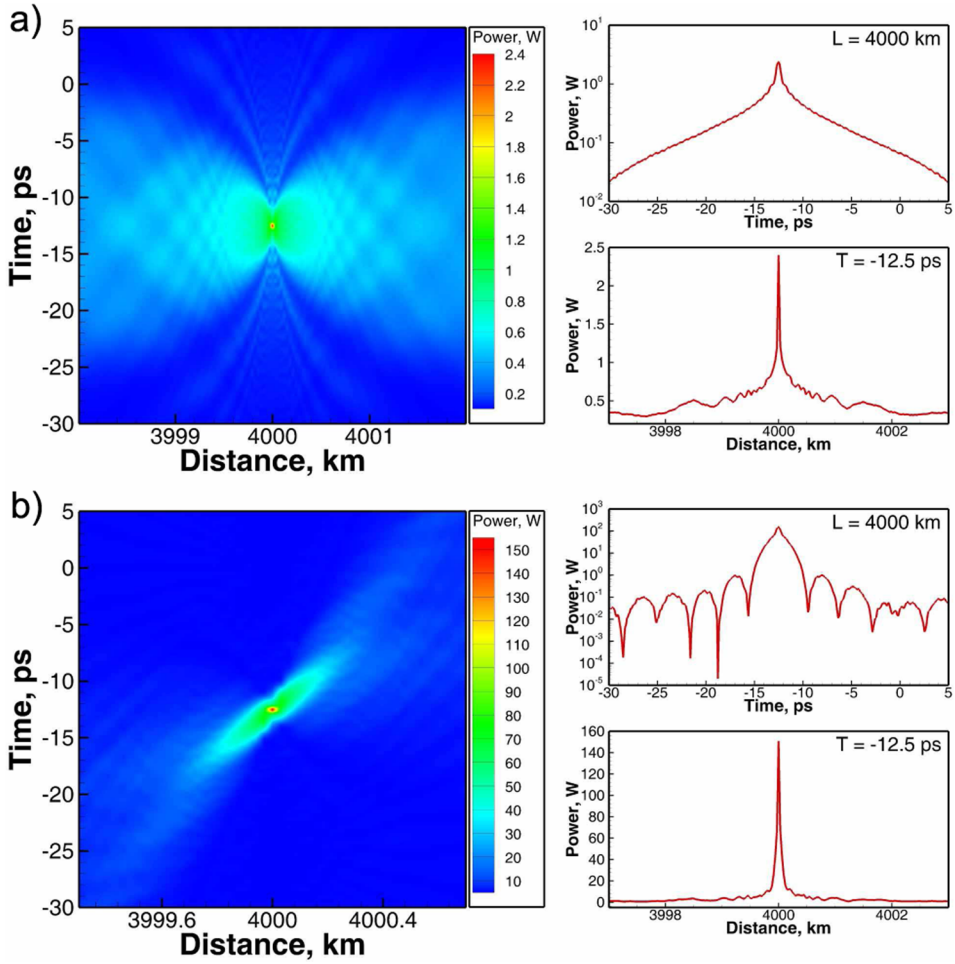

FIG. 4. Spatio-temporal dynamics of the rogue wave risen in the BPSK modulated sequence of OFDM pulses transmitted in the fiber-optic link for $N_{sc} = 1$, $N/\varphi \approx 500$ (a) and for $N_{sc} = 8$, $N/(N_{sc}\varphi) \approx 60$ (b).

dynamics of the rogue waves risen in linear mode with weak nonlinearity at the left of the figure and in nonlinear mode at the right. As is seen weak, nonlinearity leads to small shift of focus from expected distance $L = 2000$ km to the shorter one. However, it does not change either temporal or spatial shape of rogue wave, keeping it the same as in a completely linear case. Further increasing of

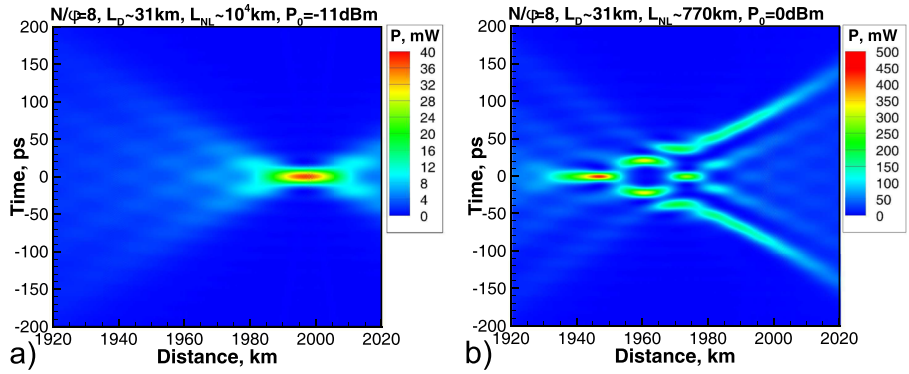

FIG. 5. Spatio-temporal dynamics of the rogue wave for weak nonlinearity mode (a) and strong nonlinearity mode (b). $N_{sc} = 1$, $N = 512$.

input signal power results in crucial transformation of the evolution of the signal, as can be seen from the right part of Fig. 5. Due to nonlinearity, a basic peak is shifted further to the left in space, forming a complex spatio-temporal pulse pattern. However, the mechanism of generation of such structures is still linear.

To estimate the influence of high amplitude fluctuations to system performance, we consider a 25 × 100 km transmission link with an ideal distributed Raman amplification (IDRA) scheme in which Raman gain exactly compensates for the fiber intrinsic loss; i.e., the signal maintains constant average power along the entire transmission length. For numerical calculations, we also use the nonlinear Schrödinger equation with addition term $N(z, t)$ on the right-hand side of Eq. (8). $N(z, t)$ corresponds to distributed amplified spontaneous emission (ASE) noise accumulation represented by a field that has the statistical properties of additive white Gaussian noise. The spectral noise density per polarization is given by $N_{ASE} = \alpha L_T n_{sp} h\nu$, where $\alpha = 0.2$ dB/km is the fiber losses, $L_T = 2500$ km is the system length, $n_{sp} = 1$ is the coefficient of the spontaneous emission, h is Planck's constant, and ν is the signal carrier frequency of 193.6 THz (1550 nm).

As an input signal we consider a 1-subcarrier QPSK-OFDM signal with two types of initial bit stream: random binary sequence and predefined binary sequence. The first one is determined by a pseudorandom process, whereas the second one is determined by (2) and (4) and leads to high power fluctuation at distance $z = 2000$ km. Transition from the optimal continuous phases to discrete phase distribution was performed by finding the closest constellation point from a discrete set of four values $\{0, \pi/2, \pi, 3\pi/2\}$. At the receiver, the chromatic dispersion was fully compensated by multiplying the Fourier transformed optical field with the reverse dispersion function. For phase estimation, an algorithm based on the 4th-power Viterbi-Viterbi method has been used. To evaluate the system performance, we use the conventional error vector magnitude (EVM) function, calculated by means of 2^{12} transmitted symbols.

Figure 6 shows the system performance as a function of signal launch power for both random and predefined bit stream. From the figure, it is seen that the optimal power difference reaches the value of 8 dB. Furthermore, occurrence and dissipation of a high power rogue wave during signal transmission results in 3 dB system performance degradation due to additive nonlinear distortion. It should be noted that the process of rogue wave generation does not depend on weak random phase

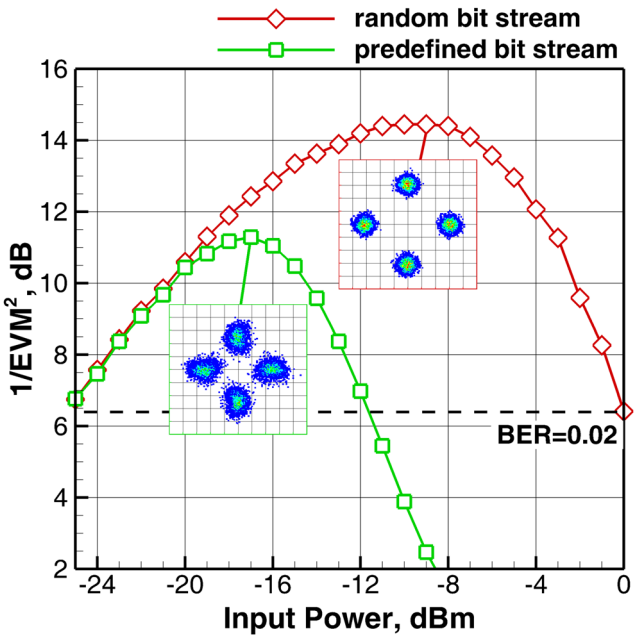

FIG. 6. System performance as a function of the signal input power for random binary sequence (red) and predefined binary sequence (green).

fluctuations because of ASE noise. It may be important for optical communication systems operating in the regime when average signal power is much greater than noise power.

CONCLUSION

In this work, we considered the visualisation of statistical fluctuations of spatio-temporal signal dynamics in long-haul transoceanic scale fiber links. A huge number of statistical realisations of spatio-temporal fluctuations in *trans*-oceanic optical systems make possible occurrences of extreme value events that might potentially affect the quality of optical signal transmission. We have identified a straightforward procedure for finding "dangerous" sequences of phase-coded symbols that lead to the occurrence of localized high power outages at certain propagation distances. We demonstrate the analogy with the rogue waves of the ocean physics and exploit similarity with the wave-front shaping methods of the diffraction optics to predict the values of the phases and describe the shape of the emerging photonic freak wave. The dispersive propagation properties of the OFDM carrier shape are shown to further enhance the effect of constructive interference of many overlapped pulses leading to the effective increase of the degrees of freedom in the phase-optimization problem. Extremely high amplitude spikes can be affected by the fiber nonlinear effects leading to signal corruption.

SUPPLEMENTARY MATERIAL

See supplementary material for the analytical derivation of the simplified OFDM transmission coefficients, the expression for the full spatio-temporal profile of the created telecom rogue wave for both OFDM and single carrier Gaussian pulses, and the exact expression for the transmission coefficients using the Fresnel diffraction theory.

ACKNOWLEDGMENTS

This work was supported by the Russian Science Foundation (Grant No. 17-72-30006).

[1] G. Proakis, *Digital Communications*, 4th ed. (McGraw-Hill, New York, 2000).
[2] W. Shieh and I. Djordjevic, *OFDM for Optical Communications* (Elesevier, Amsterdam, 2010).
[3] C. Kharif, E. Pelinovsky, and A. Slunyaev, *Rogue Waves in the Ocean* (Springer-Verlag, Berlin, 2009).
[4] I. Dyachenko and V. E. Zakharov, J. Exp. Theor. Phys. Lett. **81**, 255 (2005).
[5] D. R. Solli, C. Ropers, P. Koonath, and B. Jalali, Nature **450**, 1054 (2007).
[6] J. M. Dudley, G. Genty, and B. J. Eggleton, Opt. Express **16**, 3644 (2008).
[7] K. Hammani, C. Finot, J. M. Dudley, and G. Millot, Opt. Express **16**, 16467 (2008).
[8] N. Akhmediev, J. M. Dudley, D. R. Solli, and S. K. Turitsyn, J. Opt. **15**, 060201 (2013).
[9] N. Akhmediev, J. M. Soto-Crespo, and A. Ankiewicz, Phys. Lett. A **373**, 2137 (2009).
[10] N. Akhmediev, J. M. Soto-Crespo, and A. Ankiewicz, Phys. Rev. A **80**, 043818 (2009).
[11] A. Picozzi, J. Garnier, T. Hansson, P. Suret, S. Randoux, G. Millot, and D. N. Christodoulides, Phys. Rep. **542**, 1 (2014).
[12] S. K. Turitsyn, S. A. Babin, E. G. Turitsyna, G. E. Falkovich, E. V. Podivilov, and D. V. Churkin, in *Optical Wave Turbulence*, Advances in Wave Turbulence, edited by V. Shrira and S. Nazarenko (World Scientific, New Jersey, 2013), p. 113.
[13] E. G. Turitsyna, S. V. Smirnov, S. Sugavanam, N. Tarasov, X. Shu, S. A. Babin, E. V. Podivilov, D. V. Churkin, G. Falkovich, and S. K. Turitsyn, Nat. Photonics **7**, 783 (2013).
[14] S. Randoux, Phys. Rev. Lett. **113**, 113902 (2014).
[15] D. V. Churkin, I. V. Kolokolov, E. V. Podivilov, I. D. Vatnik, M. A. Nikulin, S. S. Vergeles, I. S. Terekhov, V. V. Lebedev, G. Falkovich, S. A. Babin, and S. K. Turitsyn, Nat. Commun. **2**, 6214 (2015).
[16] S. Vergeles and S. K. Turitsyn, Phys. Rev. A **83**, 061801(R) (2011).
[17] B. Kibler, J. Fatome, C. Finot, G. Millot, F. Dias, G. Genty, N. Akhmediev, and J. M. Dudley, Nat. Phys. **6**, 790 (2010).
[18] J. Fatome, C. Finot, G. Millot, A. Armaroli, and S. Trillo, Phys. Rev. X **4**, 021022 (2014).
[19] A. Shafarenko, K. S. Turitsyn, and S. K. Turitsyn, IEEE Trans. Commun. **55**, 237 (2007).
[20] S. J. Savory, G. Gavioli, R. I. Killey, and P. Bayvel, Opt. Express **15**, 2120 (2007).
[21] I. M. Vellekoop and A. P. Mosk, Opt. Lett. **32**, 2309 (2007).
[22] I. M. Vellekoop and A. P. Mosk, Opt. Commun. **281**, 3071 (2008).
[23] I. M. Vellekoop, A. Lagendijk, and A. P. Mosk, Nat. Photonics **4**, 320 (2010).
[24] O. Katz, E. Small, Y. Bromberg, and Y. Silberberg, Nat. Photonics **5**, 372 (2011).
[25] A. P. Mosk, A. Lagendijk, G. Lerosey, and M. Fink, Nat. Photonics **6**, 283 (2012).
[26] J. Goodman, *Speckle Phenomena in Optics* (Roberts & Co., Englewood, 2007).
[27] D. A. Coley, *An Introduction to Genetic Algorithms for Scientists and Engineers* (World Scientific, Singapore, 1999).
[28] G. Wunder, R. F. H. Fischer, H. Bochem, S. Litsyn, and J. S. No, IEEE Signal Process. Mag. **30**, 130 (2013).
[29] H. Ochai and H. Imai, IEEE Trans. Commun. **49**, 282 (2001).
[30] N. Dinur and D. Wulich, IEEE Trans. Commun. **49**, 1063 (2001).

[31] R. Schmogrow, M. Winter, M. Meyer, D. Hillerkuss, S. Wolf, B. Baeuerle, A. Ludwig, B. Nebendahl, S. Ben-Ezra, J. Meyer, M. Dreschmann, M. Huebner, J. Becker, C. Koos, W. Freude, and J. Leuthold, Opt. Express **20**, 317 (2012).
[32] R. J. Essiambre, G. Kramer, P. J. Winzer, G. J. Foschini, and B. Goebel, J. Lightwave Technol. **28**, 662 (2010).
[33] J. W. Goodman, *Introduction to Fourier Optics* (McGraw-Hill, New York, 1996).
[34] B. H. Kolner and M. Nazarathy, Opt. Lett. **14**, 630 (1989).
[35] B. H. Kolner, J. Opt. Soc. Am. A **11**, 3229 (1994).
[36] G. P. Agrawal, *The Nonlinear Fiber Optics*, 4th ed. (Academic Press, New York, 2007).
[37] J. D. Ania-Castanon, T. Ellingham, R. Ibbotson, X. Chen, L. Zhang, and S. Turitsyn, Phys. Rev. Lett. **96**, 023902 (2006).